

A Solid-State NMR and Theoretical Study of the ^{17}O Electric Field Gradient and Chemical Shielding Tensors of the Oxonium Ion in *p*-Toluenesulfonic Acid Monohydrate

Gang Wu,* Andrea Hook, Shuan Dong, and Kazuhiko Yamada

Department of Chemistry, Queen's University, Kingston, Ontario, Canada K7L 3N6

Received: December 17, 1999

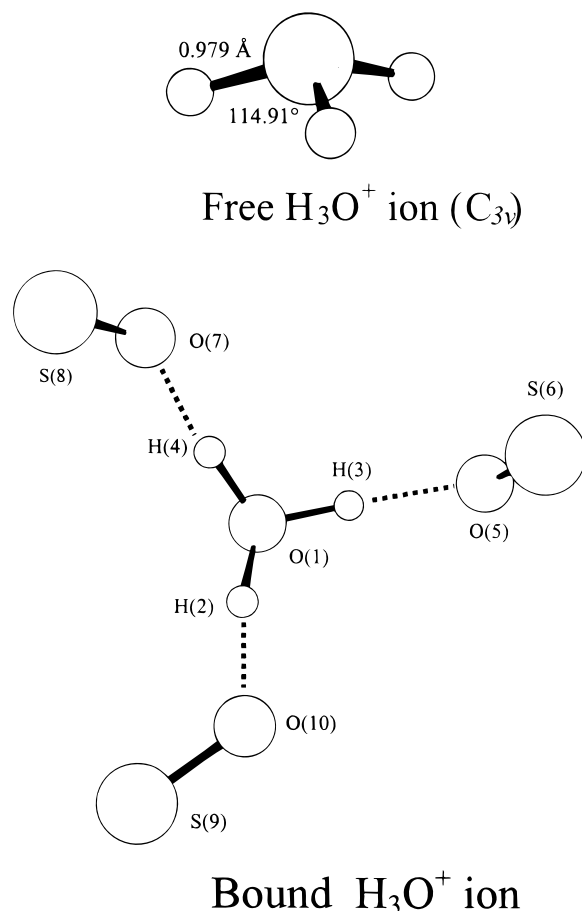
We report a solid-state ^{17}O NMR study of the ^{17}O electric field gradient (EFG) and chemical shielding (CS) tensors for the oxonium ion, H_3O^+ , in *p*-toluenesulfonic acid monohydrate (TAM). Both the ^{17}O EFG and CS tensors of the H_3O^+ ion are axially symmetric within the experimental errors. The ^{17}O quadrupole coupling constant (QCC) is found to be 7.05 ± 0.02 MHz, and the ^{17}O chemical shift anisotropy (CSA) is 87 ± 5 ppm. Experimental results are compared with extensive quantum chemical calculations using restricted Hartree–Fock approach (RHF), second-order Møller–Plesset perturbation theory (MP2), and density functional theory (DFT). The calculations showed that the strong hydrogen-bonding environment around the H_3O^+ ion in TAM is responsible for a reduction of approximately 3 MHz in the ^{17}O QCC compared to that of an isolated H_3O^+ ion. The effective ^{17}O quadrupole moment is calibrated at the B3LYP/cc-pVTZ level, $Q = -2.400$ fm². Using this value, we obtained the best calculated ^{17}O QCC for the “bound” H_3O^+ ion, +7.382 MHz, which is in reasonably good agreement with the observed value. The ^{17}O chemical shielding tensor is also calculated using the GIAO (gauge-including atomic orbital) approach. Although the calculated isotropic ^{17}O chemical shifts are in excellent agreement with the experimental data, the calculations with all the basis sets employed in the present study invariably underestimated ^{17}O CSAs by approximately 20 ppm.

I. Introduction

The hypothesis for the existence of the oxonium ion, H_3O^+ , in aqueous acid solutions can be traced back to the beginning of this century.^{1,2} However, the direct detection of H_3O^+ as a discrete ion was possible only after the advent of modern spectroscopy. An early X-ray powder diffraction study³ indicated that the solid hydrate of perchloric acid, $\text{HClO}_4 \cdot \text{H}_2\text{O}$, is isostructural with ammonium perchlorate, $\text{NH}_4^+ \text{ClO}_4^-$. This was the first indirect evidence for the existence of H_3O^+ in the crystal lattice. The definite proof of H_3O^+ came from two independent solid-state ^1H nuclear magnetic resonance (NMR) studies.⁴ Later, the geometry of H_3O^+ was established by diffraction techniques in several acid hydrates in the solid state.^{5–10} The molecular constants for a “free” H_3O^+ ion in the gas phase were reported much later by high-resolution infrared (IR) spectroscopy.¹¹ In the gas phase, the H_3O^+ ion exhibits pyramidal geometry with $r(\text{O}–\text{H}) = 0.979$ Å and $\angle\text{HOH} = 114.91^\circ$ (see Scheme 1). In the crystal lattice, the H_3O^+ ion is always involved in a three-dimensional hydrogen-bonding (HB) network. In this study, we refer to the H_3O^+ ion in a HB environment as being in the “bound” state and the isolated H_3O^+ ion as being in the “free” state.

One classic example of the “bound” H_3O^+ ion is *p*-toluenesulfonic acid monohydrate (TAM). As illustrated in Scheme 1, the H_3O^+ ion of TAM is involved in three strong $\text{O}^+–\text{H} \cdots \text{O}$ hydrogen bonds for which the $r(\text{O} \cdots \text{O})$ distances are 2.520, 2.525, and 2.538 Å.¹⁰ The “bound” H_3O^+ ion exhibits a geometry slightly distorted from C_{3v} symmetry. Compared to the geometry of a “free” H_3O^+ ion, the three O–H bonds of the “bound” H_3O^+ ion are slightly longer, 1.008, 1.013, and 1.011 Å, and the three H–O⁺–H angles are slightly larger,

SCHEME 1



* Corresponding author. Phone: 613-533-2644. Fax: 613-533-6669. E-mail: gangwu@chem.queensu.ca.

109.2, 110.7, and 109.2°, resulting in a slightly taller H_3O^+ pyramid. A previous ^1H spin–lattice relaxation study of crystalline TAM revealed a rather large activation energy, 51.6 kJ mol^{-1} , for the H_3O^+ reorientation, suggesting a strong hydrogen bonding environment.¹² Deuterium NMR was also used in the study of the H_3O^+ dynamics.^{13,14} Proton chemical shielding of the H_3O^+ ion was measured some time ago.^{15,16} The only determination of the ^{17}O quadrupole coupling constant (QCC) for the “bound” H_3O^+ ion is a nuclear quadrupole resonance (NQR) study on solid sulfuric acid monohydrate, $[\text{H}_3\text{O}^+][\text{HSO}_4^-]$, for which $e^2qQ/h = 7.513$ MHz and the asymmetry parameter $\eta = 0.104$ were observed at 77 K.¹⁷ The ^{17}O NMR parameters for the “free” H_3O^+ ion have not yet been reported.

The primary objective of the present study was to investigate how ^{17}O NMR tensors depend on the structural difference between the “free” and “bound” H_3O^+ ions. In this contribution, we report the experimental solid-state NMR determination and quantum chemical calculations of the ^{17}O electric field gradient (EFG) and chemical shielding (CS) tensors for the H_3O^+ ion in crystalline *p*-toluenesulfonic acid monohydrate.

II. Experimental Section

Toluenesulfonic acid monohydrate- ^{17}O (TAM), $4\text{-CH}_3\text{C}_6\text{H}_4\text{-SO}_3^-[\text{H}_3^{17}\text{O}]^+$, was prepared by recrystallizing 100 mg of anhydrous *p*-toluenesulfonic acid from 0.1 mL H_2^{17}O (25% ^{17}O atom, obtained from Trace Science International, Toronto, Canada). The sample was dried in a vacuum desiccator with P_2O_5 for several days. Solid-state ^{17}O NMR experiments were performed on a Bruker Avance-500 spectrometer operating at 67.80 MHz for ^{17}O nuclei. The solid sample was packed into zirconium oxide rotors (4 mm o.d.) in a glovebox under a dry N_2 environment immediately before the NMR experiment. A Bruker 4-mm double resonance probe was used in both the magic-angle spinning (MAS) and static experiments. Typical sample spinning frequencies were 10–15 kHz. No loss of hydration water was detected either during the fast MAS experiments or over a period of several days. For the static experiments, a Hahn echo sequence was used to eliminate the acoustic ringing from the probe. The rf field strength was determined using a liquid H_2O sample (25% ^{17}O atom), which was also used as an external reference sample.

III. Computational Aspects

All quantum chemical calculations were performed with the Gaussian98 program package¹⁸ on a Pentium II personal computer (400 MHz, 128 MB memory, 12 GB disk space). Due to the limitation of our computing power, a simplified model was constructed where a H_3O^+ ion is bound to three $[\text{HSO}_3]^-$ groups rather than to three *p*-toluenesulfonate groups. Thus, the model consists of a total of 19 atoms instead of 49 atoms. The crystal structure of TAM from a neutron diffraction study¹⁰ was used in our model for which no geometry optimization was performed. Since it is the interaction between H_3O^+ and SO_3^- that is most important in determining ^{17}O NMR parameters at the H_3O^+ , the simplification in our model is justified. As shown later, the good agreement between calculated and observed ^{17}O NMR parameters for TAM indicates that the simplified model is reasonable. The geometry of an isolated H_3O^+ ion was calculated with the second-order Møller–Plesset perturbation theory using the cc-pVTZ basis set.

Electric Field Gradient. Quantum chemical EFG calculations were performed using the restricted Hartree–Fock (RHF) approach, density-functional theory (DFT), and second-order

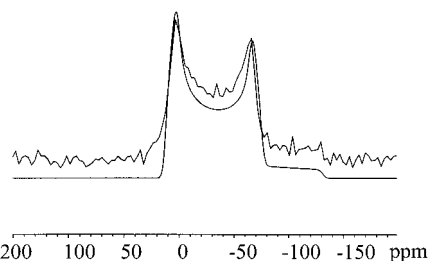


Figure 1. Experimental (upper) and simulated (lower) MAS ^{17}O NMR spectra of *p*-toluenesulfonic acid monohydrate.

Møller–Plesset perturbation theory (MP2). Five different basis sets were used: STO-3G, 6-311G, 6-311G**, TZVP, and cc-pVTZ. The principal components of the ^{17}O EFG tensor, q_{ii} , are computed in atomic units (au). In our solid-state NMR experiments, the observable quantity is the so-called quadrupole coupling tensor, χ . The two tensorial quantities are related by the following equation:

$$\chi_{ii} [\text{MHz}] = e^2Qq_{ii}/h = -2.3496Q[\text{fm}^2]q_{ii}[\text{au}] \quad (1)$$

where Q is the nuclear quadrupole moment of the ^{17}O nucleus (in units of fm^2 ; $1 \text{ fm}^2 = 10^{-30} \text{ m}^2$) and the coefficient of 2.3496 arises from the unit conversion.

Chemical Shielding. Chemical shielding calculations were performed at the RHF and DFT levels using the gauge-included atomic orbital (GIAO) method.¹⁹ Seven different basis sets were used: STO-3G, D95**, 6-311G, 6-311G**, 6-311++G**, TZVP, and cc-pVTZ. In the DFT shielding calculations, the B3LYP exchange functional²⁰ was employed.

In NMR experiments, the frequency of an NMR signal is determined relative to that arising from a standard sample. This relative quantity is known as the chemical shift, δ . In the case of ^{17}O NMR, the signal from a liquid H_2O sample is used as the chemical shift reference, $\delta(\text{H}_2\text{O}, \text{liq}) = 0$ ppm. Since quantum chemical calculations yield absolute chemical shielding values, σ , one must establish the absolute shielding scale for a particular nucleus in order to make a direct comparison between calculated results and experimental data. An accurate absolute shielding scale for ^{17}O was suggested by Wasylishen and co-workers.²¹ We used the following equation to convert the calculated ^{17}O chemical shielding values to ^{17}O chemical shifts

$$\delta = 307.9 \text{ ppm} - \sigma \quad (2)$$

where 307.9 ppm is the absolute chemical shielding constant for the ^{17}O nucleus in liquid H_2O . To describe a chemical shift tensor, we used the span (Ω) and skew (κ), in addition to the three principal components. The span and skew are related to the principal components by the following equations:²²

$$\Omega = \delta_{11} - \delta_{33} = \sigma_{33} - \sigma_{11} \quad (3)$$

$$\kappa = 3(\delta_{22} - \delta_{\text{iso}})/(\delta_{11} - \delta_{33}) = 3(\sigma_{\text{iso}} - \sigma_{22})/(\sigma_{33} - \sigma_{11}) \quad (4)$$

IV. Results and Discussion

A. Solid-State ^{17}O NMR. Figure 1 shows the central-transition ^{17}O magic-angle spinning (MAS) spectrum of TAM. The spectrum exhibits a typical line shape arising from the second-order quadrupole interaction. From the best-fit spectrum, we obtained the following ^{17}O NMR parameters: $\chi = 7.05 \pm 0.02$ MHz, $\eta = 0.0$, and $\delta_{\text{iso}} = 30.0 \pm 0.5$ ppm. The EFG tensor is axially symmetric within the experimental errors. The ^{17}O QCC value found for the H_3O^+ ion in TAM is somewhat smaller

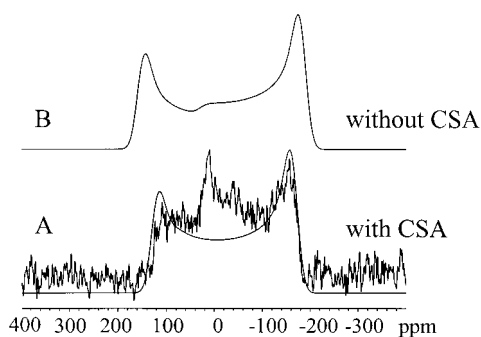


Figure 2. (A) Experimental (upper) and simulated (lower) static ^{17}O NMR spectra of *p*-toluenesulfonic acid monohydrate. (B) Simulated spectrum without ^{17}O CSA.

than that in $[\text{H}_3\text{O}^+][\text{HSO}_4^-]$ (SAM) measured at 77 K, $\chi = 7.513$ MHz.¹⁷ The different ^{17}O QCC values may be attributed to the different HB strengths of the two compounds. The H_3O^+ ion in SAM is involved in two strong and one weak $\text{O}^+-\text{H}\cdots\text{O}$ hydrogen bonds: $r(\text{O}\cdots\text{O}) = 2.54, 2.57, \text{ and } 2.65$ Å. In contrast, the three hydrogen bonds in TAM, $r(\text{O}\cdots\text{O}) = 2.520, 2.525, \text{ and } 2.538$ Å, are uniformly stronger than those in SAM. It should also be pointed out that discrepancies often exist between QCC data obtained at very different temperatures.

The isotropic ^{17}O chemical shift of H_3O^+ in TAM, $\delta_{\text{iso}} = 30$ ppm, is considerably less shielded than the previous solution ^{17}O NMR results for H_3O^+ ions, $\delta_{\text{iso}} = 9$ ppm.²³ No data are available in the literature regarding the ^{17}O CSA for H_3O^+ ions. Figure 2 shows the static ^{17}O NMR spectrum of TAM. The small sharp peak centered at approximately 10 ppm is attributed to the presence of a very small amount of liquidlike $\text{H}_3^{17}\text{O}^+$ presumably on the surface of the microcrystals as a result of the hygroscopic nature of TAM. Since the ^{17}O quadrupole parameters and the isotropic ^{17}O chemical shift have been accurately determined from the analysis of the MAS spectrum, the only remaining adjustable parameters in the simulation are the ^{17}O chemical shift anisotropy (CSA) and the relative orientation between the EFG and CS tensors. As shown in Figure 2, the best-fit line shape yields an axially symmetric CS tensor: $\delta_{11} = 88 \pm 2$ and $\delta_{22} = \delta_{33} = 1 \pm 2$ ppm. We also found that the unique component of the ^{17}O CS tensor for H_3O^+ corresponds to the direction with the least shielding, i.e., $\kappa = -1$. This is a rather unusual situation, since most ^{17}O CS tensors exhibit a positive skew.²⁴ It is somewhat interesting to note that a negative skew was also found for the nitrogen CS tensor of the NH_3 molecule,²⁵ which is isoelectronic with H_3O^+ . Furthermore, although the local molecular structure of H_3O^+ in TAM does not possess an axial symmetry,¹⁰ both the ^{17}O EFG and CS tensors of the H_3O^+ ion are axially symmetric within the experimental errors. Close examination of the crystal structure of TAM reveals that the deviation from axial symmetry is indeed negligible. As shown later, the quantum chemical calculations also confirm that the two tensors are nearly axially symmetric.

B. Quantum Chemical Calculations. To compare the ^{17}O NMR parameters between “free” and “bound” H_3O^+ ions, we first calculated the geometry of H_3O^+ in the “free” state. In Table 1, experimental and calculated molecular structures for the “free” H_3O^+ ion are summarized. Compared to the experimental structure in the gas phase, our optimized H_3O^+ geometry at the MP2/cc-pVTZ level gives a very good $r(\text{O}-\text{H})$ but a somewhat smaller $\angle\text{HOH}$. As mentioned earlier, when the H_3O^+ ion is involved in a HB network, the $\text{H}-\text{O}$ bonds lengthen slightly and the $\angle\text{HOH}$ bond angles widen. In the discussion

TABLE 1: Experimental and Calculated Molecular Structures for the H_3O^+ Ion

method	$r(\text{O}-\text{H}), \text{Å}$	$\angle\text{HOH}, \text{deg}$	ref
IR, exptl	0.979(6)	114.91(45)	11
MP2(Full)/cc-pVTZ	0.976	111.8	this work
MP2/6-31G*	0.991	111.4	26
MP2	0.977	111.2	27
MP3	0.973	111.6	27
DZ+P SCF	0.963	114.4	28
extended SCF	0.962	114.1	28
SCF	0.978	111.6	29

TABLE 2: Calculated ^{17}O EFG Values for the H_3O^+ Ion in the “Free” and “Bound” States

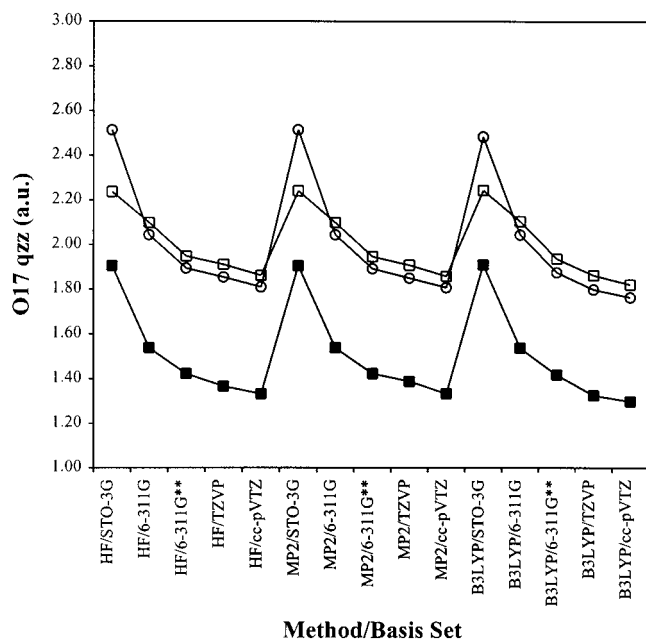
method	basis set	q_{zz} (au)		
		free ^a	free ^b	bound ^c
HF	STO-3G	2.237	2.513	1.904
	6-311G	2.098	2.043	1.537
	6-311G**	1.946	1.893	1.422
	TZVP	1.910	1.853	1.366
	cc-pVTZ	1.861	1.808	1.332
MP2(Full)	STO-3G	2.240	2.513	1.904
	6-311G	2.098	2.043	1.538
	6-311G**	1.944	1.890	1.422
	TZVP	1.906	1.849	1.387
	cc-pVTZ	1.857	1.807	1.332
B3LYP	STO-3G	2.243	2.484	1.908
	6-311G	2.105	2.044	1.536
	6-311G**	1.936	1.875	1.416
	TZVP	1.861	1.797	1.325
	cc-pVTZ	1.820	1.763	1.298

^a Optimized structure at the MP2/cc-pVTZ level. ^b Neutron diffraction geometry. ^c Neutron diffraction structure of *p*-toluenesulfonic acid monohydrate.

that follows, we will discuss the EFG and chemical shielding calculations separately.

The Electric Field Gradient Tensor. Extensive quantum chemical calculations were performed in order to evaluate the effect of strong HB interactions on the ^{17}O EFG tensor. The calculated EFG results are presented in Table 2. For the ^{17}O EFG calculations on the “free” H_3O^+ ion, we used two sets of geometry, the optimized structure and the geometry from the neutron diffraction study of TAM. By comparing these calculations with the result of a completely “bound” H_3O^+ ion, it should be possible to assess to what extent the subtle structural change at the H_3O^+ ion itself contributes to the change of the EFG at the central oxygen nucleus.

The calculated EFG data are plotted in Figure 3, from which several trends are clearly observed. First, the use of larger basis sets always results in smaller ^{17}O EFG values. As seen from Figure 3, the EFG value converges at the cc-pVTZ level, regardless of the method used in the calculations. Second, the ^{17}O EFG at the oxygen nucleus is significantly reduced in the “bound” state, in which three strong hydrogen bonds are present. All three levels of theory predicted an approximately 25–28% reduction in the ^{17}O QCC value. This is similar to the situation for H_2O , for which Butler and Brown³⁰ also predicted a large reduction of ^{17}O EFG in strong hydrogen-bonded systems. Third, with the exception of the STO-3G data, there exists very little difference between the EFG values for the “free” H_3O^+ ions with either the optimized geometry or the neutron diffraction structure. This observation suggests that the subtle structural change of the H_3O^+ moiety accounts for less than 10% of the total ^{17}O EFG reduction between the “free” and “bound” H_3O^+ ions. Clearly, the presence of the HB acceptors, SO_3^- , is largely responsible for the observed ^{17}O EFG value in the “bound” state.



Method/Basis Set

Figure 3. Plot illustrating the method/basis set dependence of the calculated ^{17}O EFG for the “free” and “bound” H_3O^+ ions: (□) “free” H_3O^+ ions with the optimized geometry, (○) “free” H_3O^+ ions with the neutron diffraction geometry, (■) “Bound” H_3O^+ ions with the neutron diffraction geometry.

TABLE 3: Experimental and Calculated (B3LYP/cc-pVTZ) ^{17}O EFG Values for Small Molecules^a

molecule	experimental χ (MHz)	calculated q_{zz} (au)	calculated χ (MHz) ^b
H_2CO^c	12.35	2.145	12.096
MeOH^d	11	1.941	10.945
$\text{H}_2\text{O}(\text{g})^e$	10.1068	1.861	10.494
SO_2^f	6.6	1.237	6.976
CO^g	4.337	0.762	4.298
HNCO^h	3.452	0.739	4.168
SCO^i	-1.32	-0.219	-1.235
O_2^j	-8.42	-1.394	-7.861

^a All calculations were based on the microwave structures. ^b The calibrated ^{17}O quadrupole moment, Q , was -2.400 fm^2 at the B3LYP/cc-pVTZ level. ^c From ref 34. ^d From ref 35. ^e From ref 36. ^f From ref 37. ^g From ref 38. ^h From ref 39. ⁱ From ref 40. ^j From ref 41.

In the above discussion, we have focused on the calculated EFG values. Experimentally, what we determined is the quadrupole coupling constant, QCC. To compare the calculated EFG results with the observed QCC, it is necessary to know the ^{17}O nuclear quadrupole moment, Q (see eq 1). Since the literature values for $Q(^{17}\text{O})$ vary about 30%, it is difficult to compare directly the calculated EFG results with the observed QCC value. Recently, several groups demonstrated a calibration approach, based on which an effective ^{17}O quadrupole moment can be derived for a particular level of theory.^{31–33} The proposed calibration procedure consists of three steps. First, one selects a group of small molecules for which accurate values of ^{17}O QCCs have been determined by high-resolution microwave spectroscopy. Second, one calculates the EFG values for these small molecules at a particular level of theory. Finally, one adjusts the value of Q to minimize the errors between the calculated QCC values and the observed data using eq 1. Following this procedure, we calibrated the effective Q at the B3LYP/cc-pVTZ level. The results are shown in Table 3 and plotted in Figure 4. As seen from Figure 4, the B3LYP/cc-pVTZ calculation can produce reliable ^{17}O EFG results when using an effective Q of -2.400 fm^2 . This value is consistent with the

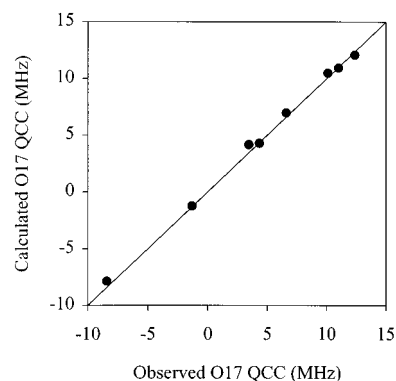


Figure 4. Calculated and observed ^{17}O QCC values for several small molecules; see Table 3.

effective Q values calibrated at similar levels of theory.^{31–33} Using this value, we found $\chi(\text{B3LYP/cc-pVTZ}) = 7.382 \text{ MHz}$ for the “bound” H_3O^+ ion, which is in reasonably good agreement with the experimental value, 7.05 MHz. It should be noted that the sign of χ cannot be directly determined from our solid-state ^{17}O NMR experiments. For a “free” H_3O^+ ion, the B3LYP/cc-pVTZ calculations yielded $\chi = 10.352 \text{ MHz}$. A positive χ value is consistent with a previous determination for the H_3O^+ ion in sulfuric acid monohydrate.¹⁷

The Chemical Shielding Tensor. As mentioned in the previous section, the EFG at the oxygen nucleus of H_3O^+ is remarkably sensitive to the HB interaction. In this section, we will focus on the HB effect on the ^{17}O chemical shielding. Calculated ^{17}O chemical shielding tensors for both the “free” and “bound” H_3O^+ ions are summarized in Table 4. For the “free” H_3O^+ ion, the calculated isotropic ^{17}O chemical shielding constants are in agreement with a theoretical value previously reported by Chesnut, 306.6 ppm.⁴² The calculated ^{17}O shielding tensors for the free H_3O^+ ion are axially symmetric, as required by the C_{3v} molecular symmetry. For the “bound” H_3O^+ ions, although there is no symmetry requirement, the calculated ^{17}O chemical shielding tensors are nearly axially symmetric. This is in agreement with the experimental finding mentioned earlier.

The chemical shielding calculations at both the RHF and DFT levels also reveal that the oxygen nucleus of the H_3O^+ ion is less shielded by ca. 40 ppm in the “bound” state than in the “free” state, as illustrated in Figure 5A. This discrepancy is attributed to the HB interaction. This trend has been observed in ^{17}O NMR for compounds with singly bonded oxygen atoms. For example, the ^{17}O NMR signal for gaseous H_2O appears at $\delta = -36.1 \text{ ppm}$ with respect to that of liquid water.²¹ Interestingly, the calculations seem to start to converge at the Dunning full double- ζ basis set with polarization functions, D95**.*. Our recent studies on the amide oxygen chemical shielding tensors also indicated that the B3LYP/D95**.* calculations can reproduce reasonably well the experimental ^{17}O chemical shielding tensors, provided that a complete HB network was included in the calculation.⁴³ However, comparison between the calculated and observed isotropic chemical shift values alone might be misleading. As shown in Figure 5B, although the calculated isotropic ^{17}O chemical shifts are in excellent agreement with the observed value, the calculated ^{17}O CSAs exhibit large discrepancies from the experimental result. The calculations constantly underestimate the ^{17}O CSA for the “bound” H_3O^+ ion, even with the very extensive basis sets. This suggests that the uncertainty in the present quantum chemical ^{17}O shielding calculations is on the order of 20 ppm, rather than the 3 ppm uncertainty suggested by comparing the isotropic chemical shifts alone. This example illustrates the importance

TABLE 4: Calculated ^{17}O Chemical Shielding Tensors for the H_3O^+ Ion in the “Free” and “Bound” States

method	basis set	free H_3O^+ ^a			bound H_3O^+ ^b				
		σ_{iso}	σ_{\parallel}	σ_{\perp}	σ_{iso}	σ_{11}	σ_{22}	σ_{33}	
HF	STO-3G	386.2	359.4	399.6	404.1	377.6	415.7	419.0	
	D95**	321.5	296.9	333.9	293.3	263.8	306.8	309.8	
	6-311G	318.4	290.2	333.0	293.8	260.98	306.5	313.9	
	6-311G**	314.0	284.5	328.8	292.3	257.0	308.5	311.4	
	6-311++G**	309.2	282.9	322.4	279.2	249.9	293.7	294.1	
	TZVP	311.1	284.8	324.2	283.9	253.4	298.6	299.7	
	cc-pVTZ	310.9	283.8	324.5	285.3	253.4	300.1	302.2	
B3LYP	STO-3G	366.0	340.5	378.8	378.3	350.0	390.2	394.5	
	D95**	312.8	284.6	326.8	272.9	238.9	287.6	292.4	
	6-311G	312.1	277.5	329.4	278.0	238.7	292.4	302.9	
	6-311G**	309.8	274.0	327.7	276.6	233.9	295.4	300.5	
	6-311++G**	303.1	272.0	318.6	258.8	225.6	275.1	275.8	
	TZVP	305.8	274.9	321.2	265.9	230.3	282.4	285.1	
	cc-pVTZ	305.8	273.6	321.8	266.8	228.6	284.3	287.6	

^a Optimized structure at the MP2(Full)/cc-pVTZ level. ^b Neutron diffraction structure of *p*-toluenesulfonic acid monohydrate.

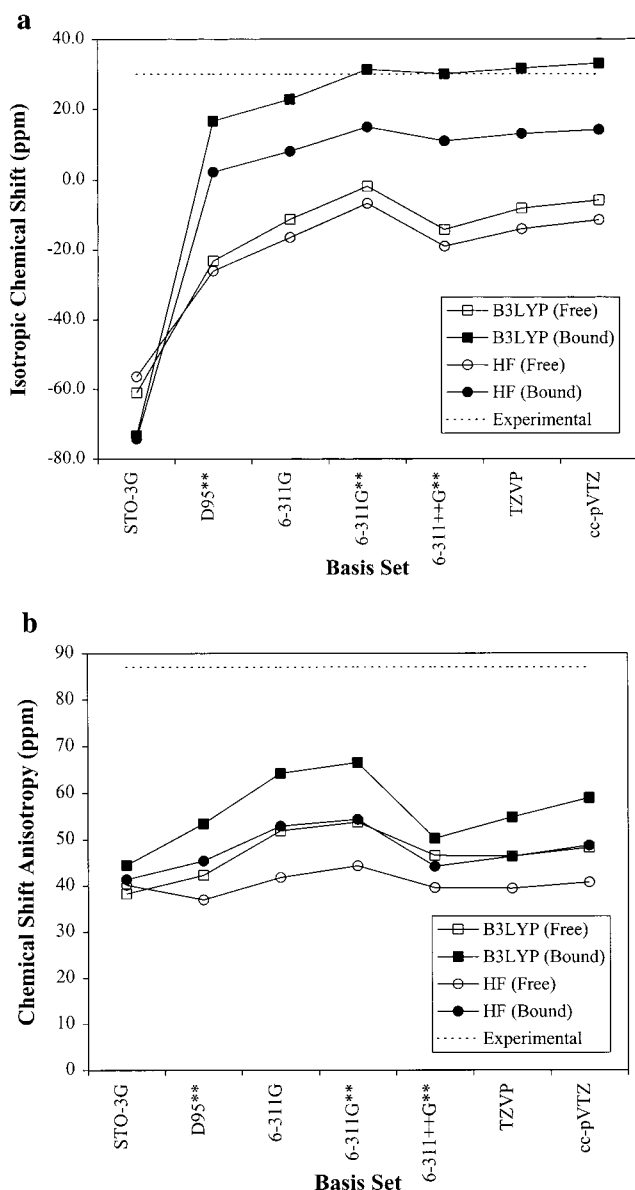


Figure 5. Experimental (dotted line) and calculated (solid line) ^{17}O isotropic chemical shifts (A) and CSAs (B) for the “free” and “bound” H_3O^+ ions.

of examining the complete chemical shielding tensor. It is noted that a previous IGLO (individual gauge for localized orbital) calculation⁴⁴ yielded a similar ^{17}O CSA for the “free” H_3O^+

ion, $\Omega = 51.0$ ppm. On the basis of the present theoretical data, we can conclude that the B3LYP approach always generates better ^{17}O NMR tensors for the H_3O^+ ions than does the RHF method. However, the accuracy of the ^{17}O chemical shielding calculations at the present levels of theory is not completely satisfactory. Since the “bound” H_3O^+ ion in TAM has approximately 3-fold symmetry, any molecular 3-fold jump motion on the NMR time scale will have negligible effects on the observed ^{17}O EFG and CS tensors. The discrepancy between the calculated and observed ^{17}O NMR parameters is believed to arise partly from the simplified model and partly from the limitation of the present theoretical approach. Perhaps higher levels of theory such as the GIAO-CCSD(T) approach may be able to improve the accuracy of the ^{17}O chemical shielding calculation.⁴⁵

V. Conclusions

We have reported a solid-state ^{17}O NMR study for the oxonium ion, H_3O^+ , in crystalline TAM. Using the experimental data, we have evaluated the reliability of modern quantum chemical calculations at various levels of theory. The calculations revealed that both the ^{17}O EFG and CS tensors are remarkably sensitive to hydrogen-bonding interactions. In particular, the presence of three strong $\text{O}^+-\text{H}\cdots\text{O}$ hydrogen bonds in crystalline TAM is responsible for the significantly reduced ^{17}O QCC and the increased isotropic chemical shielding constant at the oxygen nucleus of the H_3O^+ ion, compared to those for a free H_3O^+ ion. However, the ^{17}O CSA of the “bound” H_3O^+ ion is only slightly larger than that for a free H_3O^+ ion. The ^{17}O EFG calculations at the B3LYP/cc-pVTZ level reproduced very well the experimental ^{17}O QCC value. Although the ^{17}O chemical shielding calculations at the same level of theory yielded an isotropic ^{17}O chemical shielding constant, in excellent agreement with the observed value, the calculated ^{17}O CSAs were invariably too small by approximately 20 ppm. The benchmark experimental values of the ^{17}O EFG and CS tensors determined for the “free” and “bound” H_3O^+ ions will be useful in the testing of future quantum chemical calculations, especially regarding to methodologies in handling strong hydrogen-bonding interactions.

Acknowledgment. This research was supported by the Natural Sciences and Engineering Research Council (NSERC) of Canada. We wish to thank Dr. Minhuy Ho for assistance with the Gaussian98 program. A.H. thanks NSERC for a Summer Research Scholarship. We are also grateful to Professor

John A.S. Smith for directing us to the ¹⁷O NQR reference (ref 17) and to an anonymous reviewer for very helpful comments.

References and Notes

- (1) Giguère, P. A. *J. Chem. Ed.* **1979**, *56*, 571.
- (2) Ratcliffe, C. I.; Irish, D. E. In *Water Science Review 2: Crystalline Hydrates*; Franks, F., Ed.; Cambridge University Press: Cambridge, U.K., 1986; p 149.
- (3) Volmer, M. *Ann. Chem.* **1924**, *440*, 200.
- (4) Richards, R. E.; Smith, J. A. S. *Trans. Faraday Soc.* **1951**, *47*, 1261. (b) Kakiuchi, Y.; Shono, H.; Komatsu, H.; Kigoshi, K. *J. Chem. Phys.* **1951**, *19*, 1069.
- (5) Young, K. Y.; Carpenter, G. B. *Acta Crystallogr.* **1959**, *12*, 17.
- (6) Lee, F. S.; Carpenter, G. B. *J. Chem. Phys.* **1959**, *63*, 279.
- (7) Nordman, C. E. *Acta Crystallogr.* **1962**, *15*, 18.
- (8) Taesler, I.; Olovsson, I. *Acta Crystallogr.* **1968**, *B24*, 299.
- (9) Arora, S. K.; Sundaralingam, M. *Acta Crystallogr.* **1971**, *B27*, 1293.
- (10) Lundgren, J.-O.; Williams, J. M. *J. Chem. Phys.* **1973**, *58*, 788.
- (11) Begemann, M. H.; Gudeman, C. S.; Pfaff, J.; Saykally, R. *J. Phys. Rev. Lett.* **1983**, *51*, 554.
- (12) Ratcliffe, C. I.; Dunell, B. A. *J. Chem. Soc., Faraday Trans. 2*, **1981**, *77*, 2181.
- (13) O'Reilly, D. E.; Peterson, E. M.; Williams, J. M. *J. Chem. Phys.* **1971**, *54*, 96.
- (14) Ratcliffe, C. I. *J. Phys. Chem.* **1994**, *98*, 10935.
- (15) Ratcliffe, C. I.; Ripmester, J. A.; Tse, J. S. *Chem. Phys. Lett.* **1985**, *120*, 427.
- (16) Sears, R. E. J.; Kaliaperumal, R.; Ratcliffe, C. I. *J. Chem. Phys.* **1990**, *93*, 2959.
- (17) Pople, I. J. *J. Magn. Reson.* **1981**, *44*, 488.
- (18) Frisch, M. J.; Trucks, G. W.; Schlegel, H. B.; Scuseria, G. E.; Robb, M. A.; Cheeseman, J. R.; Zakrzewski, V. G.; Montgomery, J. A.; Stratmann, R. E.; Burant, J. C.; Dapprich, S.; Millam, J. M.; Daniels, A. D.; Kudin, K. N.; Strain, M. C.; Farkas, O.; Tomasi, J.; Barone, V.; Cossi, M.; Cammi, R.; Mennucci, B.; Pomelli, C.; Adamo, C.; Clifford, S.; Ochterski, J.; Petersson, G. A.; Ayala, P. Y.; Cui, Q.; Morokuma, K.; Malick, D. K.; Rabuck, A. D.; Raghavachari, K.; Foresman, J. B.; Cioslowski, J.; Ortiz, J. V.; Baboul, A. G.; Stefanov, B. B.; Liu, G.; Liashenko, A.; Piskorz, P.; Komaromi, I.; Gomperts, R.; Martin, R. L.; Fox, D. J.; Keith, T.; Al-Laham, M. A.; Peng, C. Y.; Nanayakkara, A.; Gonzalez, C.; Challacombe, M.; Gill, P. M. W.; Johnson, B.; Chen, W.; Wong, M. W.; Andres, J. L.; Head-Gordon, M.; Replogle, E. S.; Pople, J. A. *Gaussian 98, Revision A.7*, Gaussian, Inc.: Pittsburgh, PA, 1998.
- (19) Ditchfield, R. *Mol. Phys.* **1974**, *27*, 789. (b) Wolinski, K.; Hilton, J. F.; Pulay, P. *J. Am. Chem. Soc.* **1990**, *112*, 8257.
- (20) Becke, A. D. *Phys. Rev.* **1988**, *A38*, 3098. (b) Lee, C.; Yang, W.; Parr, R. G. *Phys. Rev.* **1988**, *B37*, 785. (c) Becke, A. D. *J. Chem. Phys.* **1993**, *98*, 5648.
- (21) Wasylishen, R. E.; Mooibroek, S.; Macdonald, J. B. *J. Chem. Phys.* **1984**, *81*, 1057.
- (22) Mason, J. *Solid State Nucl. Magn. Reson.* **1993**, *2*, 285.
- (23) Mateescu, G. D.; Benedikt, G. M. *J. Am. Chem. Soc.* **1979**, *101*, 3959. (b) Olah, G. A.; Berrier, A. L.; Prakash, G. K. S. *J. Am. Chem. Soc.* **1982**, *104*, 2373.
- (24) Duncan, T. M. *Chemical Shift Tensors*, 2nd ed.; The Farragut Press: Madison, WI, 1997.
- (25) Kukolich, S. G.; Wofsy, S. C. *J. Chem. Phys.* **1970**, *52*, 5477. (b) Appleman, B. R.; Dailey, B. P. *Adv. Magn. Reson.* **1974**, *7*, 149.
- (26) Olah, G. A.; Burcher, A.; Rasul, G.; Gnann, R.; Christe, K. O.; Prakash, G. K. S. *J. Am. Chem. Soc.* **1997**, *119*, 8035.
- (27) Rodwell, W. R.; Radom, L. *J. Am. Chem. Soc.* **1981**, *103*, 2865.
- (28) Colvin, M. E.; Raine, G. P.; Schaefer, H. F., III; Dupuis, M. *J. Chem. Phys.* **1983**, *79*, 1551.
- (29) Bunker, P. R.; Kraemer, W. P.; Špirko, V. *J. Mol. Spectrosc.* **1983**, *101*, 180.
- (30) Butler, L. G.; Brown, T. L. *J. Am. Chem. Soc.* **1981**, *103*, 6541.
- (31) Eggenberger, R.; Gerber, S.; Huber, H.; Searles, D.; Welker, M. *J. Mol. Spectrosc.* **1992**, *151*, 474.
- (32) Ludwig, R.; Weinhold, F.; Farrar, T. C. *J. Chem. Phys.* **1995**, *103*, 6941; **1996**, *105*, 8223.
- (33) De Luca, G.; Russo, N.; Köster, A. M.; Calaminici, P.; Jug, K. *Mol. Phys.* **1999**, *97*, 347.
- (34) Cornet, R.; Landsberg, B. M.; Winnewisser, G. *J. Mol. Spectrosc.* **1980**, *82*, 253.
- (35) Palmer, M. H. *Z. Naturforsch.* **1996**, *51A*, 442.
- (36) (a) Verhoeven, J.; Dymann, A.; Bluysen, H. *J. Chem. Phys.* **1969**, *50*, 3330. (b) Bellet, J.; Lafferty, W. J.; Steenbeckelers, G. *J. Mol. Spectrosc.* **1973**, *47*, 388. (c) De Lucta, F. C.; Helminger, P. *J. Mol. Spectrosc.* **1975**, *56*, 138.
- (37) Wasylishen, R. E.; Macdonald, J. B.; Friedrich, J. O. *Can. J. Chem.* **1984**, *62*, 1181.
- (38) Frerking, M. A.; Langer, W. D. *J. Chem. Phys.* **1981**, *74*, 6990.
- (39) Gerry, M. C. L.; Howard, S. J.; Heineking, N.; Dreizler, H. Z. *Naturforsch.* **1989**, *44A*, 1187.
- (40) Merke, I.; Dreizler, H. Z. *Naturforsch.* **1987**, *42A*, 1043.
- (41) Gerber, P. *Helv. Phys. Acta* **1972**, *45*, 655.
- (42) Chesnut, D. B. *Annu. Rep. NMR Spectrosc.* **1989**, *21*, 51.
- (43) Wu, G.; Yamada, K.; Dong, S.; Grondy, H. *J. Am. Chem. Soc.* In press.
- (44) Kutzelnigg, W.; Fleischer, U.; Schindler, M. In *NMR—Basic Principles and Progress*; Springer-Verlag: Berlin, 1990; Vol. 23, p 165.
- (45) Gauss, J.; Stanton, J. F. *J. Chem. Phys.* **1996**, *104*, 2574.